Phycological Research

Phycological Research 2015; **63:** 19–28 doi: 10.1111/pre.12072

Multiple losses of photosynthesis in *Nitzschia* (Bacillariophyceae)

Ryoma Kamikawa,[1,2]* Naoji Yubuki,[6] Masaki Yoshida,[3] Misaka Taira,[3] Noriaki Nakamura,[4] Ken-ichiro Ishida,[3] Brian S. Leander,[6] Hideaki Miyashita,[1,2] Tetsuo Hashimoto,[3,4] Shigeki Mayama[5] and Yuji Inagaki[3,4]

[1]Graduate School of Global Environmental Studies, [2]Graduate School of Human and Environmental Studies, Kyoto University, Kyoto, [3]Graduate School of Life and Environmental Sciences, [4]Center for Computational Sciences, University of Tsukuba, Tsukuba, [5]Department of Biology, Tokyo Gakugei University, Tokyo, Japan, and [6]Departments of Zoology and Botany, University of British Columbia, Vancouver, British Columbia, Canada

SUMMARY

In order to obtain insights into the evolution of colorless (apochlorotic) diatoms, we investigated newly established apochlorotic strains of *Nitzschia* spp. using light and electron microscopy and molecular phylogenetic analyses. Fluorescence microscopic observations demonstrated that the apochlorotic diatoms lack chlorophylls. Transmission electron microscopy of two apochlorotic strains also demonstrated that their plastids lacked thylakoids; instead, having four-membrane-bound organelles without thylakoids, similar to nonphotosynthetic plastid remnants. From the apochlorotic strains, we also found plastid small subunit rRNA genes that were unusually long branched in phylogenetic analyses, as observed in other nonphotosynthetic plastids. Molecular phylogenetic analysis of the nucleus-encoded large subunit rRNA genes showed eight distinct lineages for apochlorotic diatoms. The eight apochlorotic lineages were not monophyletic, suggesting that the loss of photosynthesis took place multiple times independently within *Nitzschia*. Several diatoms, including *Nitzschia* spp., are mixotrophic, which is an expected mode of nutrition that would help explain the evolutionary switch from a photosynthetic lifestyle to a heterotrophic lifestyle.

Key words: apochlorotic diatoms, genetic diversity, large subunit rRNA, molecular phylogenetic analysis, nonphotosynthetic plastids, plastid 16S rRNA.

INTRODUCTION

Diatoms comprise the most species-rich group of algae and play important ecological roles as primary producers in aquatic environments. It is reported that diatoms contribute up to 20% of global net primary production (Field *et al*. 1998; Mann 1999). In addition to this beneficial contribution to ecosystems, some diatoms can also form harmful red tides and disrupt economically important industries such as fisheries (Anderson 1989; Hallegaeff 1993).

Most diatoms are photosynthetic, and only seven species are known to be obligate heterotrophs: *Hantzschia achroma* Li and Volcani, *Nitzschia alba* Lewin and Lewin, *N. albicostalis* Li and Volcani, *N. fluorescens* Li and Volcani, *N. leucosigma* Benecke, *N. lucisensibilis* Li and Volcani, and *N. putrida* (Cohn) Benecke (Benecke 1900, Lewin & Lewin 1967; Li & Volcani 1987). These apochlorotic diatoms live on different macroalgae such as *Sargassum* sp., *Fucus* sp., *Pelagophycus* sp., *Hesperophycus harveyanus* (Decaisne) Setchell & N.L.Gardner, *Macrocystis pyrifera* (Linnaeus) C.Agardh, *Enteromorpha* sp., *Zostera* sp., *Codium fragile* (Suringar) Hariot, and *Phyllospadix torreyi* S.Watson (e.g., Lewin & Lewin 1967; Li & Volcani 1987). In addition, apochlorotic diatoms have also been found in mangroves and intertidal sand (Blackburn *et al*. 2009a,b). Apochlorotic diatoms are inferred to have lost photosynthesis secondarily, because most diatoms and their nearest relatives, such as the Bolidophyceae (Daugbjerg & Guillou 2001), are photosynthetic. Lauritis *et al*. (1968) and Schnepf (1969) observed non-photosynthetic plastids in *Nitzschia alba* using transmission electron microscopy (TEM).

Six out of the seven known species of apochlorotic diatoms belong to *Nitzschia*, which are ubiquitous pennate diatoms including more than 1000 species. Lauritis *et al*. (1967) and Geitler (1968) reported that *Hantzschia*-like cells are produced by some *Nitzschia* species, which calls into question the traditional separation of these two genera (Mann 1980; Pickett-Heaps 1983). Molecular phylogenetic analyses show that the type species of *Hantzschia*, *H. amphioxys* (Ehrenberg) Grunow, is nested within the *Nitzschia* clade (e.g., Trobajo *et al*. 2009). Apochlorotic diatoms reported so far are not broadly distributed across the tree of diatoms, but are restricted to only one subgroup consisting of *Nitzschia* and *Hantzschia*. However, because the phylogenetic relationships amongst apochlorotic diatoms remain unclear, we cannot trace the evolutionary history associated with the loss of photosynthesis in diatoms. In this study, we addressed the evolution of apochlorotic diatoms by establishing 22 cultures of apochlorotic *Nitzschia* spp. and inferring their molecular phylogenetic relationships.

MATERIALS AND METHODS

Collection and maintenance of cultures

Water samples and mangroves leaves of *Bruguiera gymnorrhiza* (L.) Lamk. and *Rhizophora mucronata* Lamk.

*To whom correspondence should be addressed.
Email: kamikawa.ryoma.7v@kyoto-u.ac.jp
Communicating editor: Giuseppe C. Zuccarello
Received 10 January 2014; accepted 17 July 2014.

Table 1. Strains used in this study

Strains	Morpho-types†	Phylo-types‡	Origins	Nuclear LSU rRNA gene§	Plastid 16S rRNA gene§
IriIs01	A	Lineage 1	Iriomote Island	AB899687	–
IriIs02	A	Lineage 1	Iriomote Island	AB899690	AB899711
IriIs03	A	Lineage 1	Iriomote Island	AB899688	AB899708
IriIs04	A	Lineage 1	Iriomote Island	AB899689	AB899709
IriIm01	A	Lineage 1	Iriomote Island	AB899691	AB899710
IriIL01	A	Lineage 1	Iriomote Island	AB899701	AB899712
IriSm01	C	Lineage 3	Iriomote Island	AB899686	AB899718
IriSm02	C	Lineage 3	Iriomote Island	AB899699	AB899719
IriSL01	E	Lineage 5	Iriomote Island	AB899700	–
IriSs06	D	Lineage 4	Iriomote Island	AB899692	AB899728
A4	F	Lineage 6	Ishigaki Island	AB899702	AB899716
B3	F	Lineage 6	Ishigaki Island	AB899703	AB899717
C2	C	Lineage 3	Ishigaki Island	AB899704	AB899720
D2	E	Lineage 5	Ishigaki Island	AB899705	AB899721
D3	A	Lineage 1	Ishigaki Island	AB899706	AB899722
E1	A	Lineage 1	Ishigaki Island	AB899707	AB899723
I4	B	Lineage 2	Ishigaki Island	AB899693	AB899715
K1	B	Lineage 2	Ishigaki Island	AB899694	AB899714
K2	B	Lineage 2	Ishigaki Island	AB899695	AB899713
M1	F	Lineage 6	Ishigaki Island	AB899696	AB899727
N4	F	Lineage 6	Ishigaki Island	AB899697	AB899726
O2	A	Lineage 1	Ishigaki Island	AB899698	AB899725

†Corresponding with Figure 1, ‡Corresponding with Figure 5, §GenBank accession numbers. –, Not amplified by PCR.

Table 2. Morphological characters for apochlorotic diatoms used

Morphotypes†	Valve faces	Girdle faces	Keel puncta/ 10 μm
A (IriIs04)	Lanceolate	Rectangular	15–18
B (K1)	Fusiform	Sigmoid	14–18
C (IriSm01)	Fusiform with slightly sigmoid end	Sigmoid	12–14
D (IriSs06)	Wide lanceolate/scalpelliform	Rectangular	12–14
E (IriSL01)	Linear with slightly sigmoid end	Sigmoid	12–15
F (B3)	Linear/scalpelliform	Sigmoid	12–14

†Corresponding with Figure 1. Strains used are shown in parentheses.

were collected from Iriomote Island (123°76′ E, 24°39′ N; 123°78′ E, 24°40′ N; 123°81′ E, 24°40′ N) and Ishigaki Island (124°13′ E, 24°47′ N; 124°21′ E, 24°36′ N; 124°23′ E, 24°48′ N) in Okinawa, Japan, and each of these samples was inoculated in autoclaved seawater and maintained at 20°C under dark conditions. Single cells of colorless *Nitzschia* spp. were isolated by micro-pipetting and cultured on a seawater-based Glucose Yeast Peptone Agar plate (1 L autoclaved seawater including 15 g agarose, 2 g glucose, 0.5 g Yeast extract, 1 g Peptone, 0.05 g kanamycin, and 0.05 g ampicillin) followed by further incubation under dark conditions. The plating procedures were repeated at least three times for each single colony in order to establish pure colonies. Established culture strains were also maintained at 20°C in Erd-Schreiber Modified medium (Kasai *et al.* 2009) using a 14 h light:10 h dark cycle. The strains used in this study are summarized in Tables 1 and 2. Strains IriIs01, IriIs03, IriIs04, IriSL01, A4, B3, and N4 were deposited to the National Institute for Environmental Study (NIES; Tsukuba, Japan) with no. NIES-3579, NIES-3580, NIES-3581, NIES-3582, NIES-3576, NIES-3577, and NIES-3579, respectively. Voucher slides for strain IriIs04, IriSm01, IriSL01, IriSs06, B3, and K1 were deposited as sample nos. TNS-AL-55697, TNS-AL-56998, TNS-AL-55696, TNS-AL-56999, TNS-AL-55698, and TNS-AL-55699, respectively, in TNS (Department of Botany, National Museum of Nature and Science, Tsukuba, Japan).

Light microscopy

For all but one strain, living cells were observed with a light microscope (Axioskop; Zeiss, Oberkochen, Germany) and the images were captured by a digital camera (DP71; Olympus, Tokyo, Japan). The cleaned frustules were prepared following Nagumo (1995). Otherwise, cells were exposed to low temperature plasma as described in Watanabe *et al.* (2010). Cleaned specimens were mounted in Pleurax (Wako Pure Chemical Industries, Osaka, Japan) followed by a light microscope (SKE; Nikon, Tokyo, Japan) equipped with a digital camera (Infinity1-5-M; Lumenera, Ottawa, Canada).

Fluorescence and electron microscopy

For fluorescence microscopy, the cells were observed using an epifluorescence microscope (BX51N-34-FLD-1; Olympus) under bright field, UV, and green excitation, after staining with 0.1% 4′, 6-diamidino-2-phenylindole (DAPI) (Porter & Feig 1980) without fixation.

For TEM observations, cell suspensions in media were mixed with an equal volume of fixative [2.5% glutaraldehyde and 0.25 M sucrose in 0.05 M sodium cacodylate buffer (pH 7.2)] at 4°C for 2 h. Cells were then rinsed several times with the same buffer and post-fixed with 1% osmium tetroxide for 30 min. The cells were dehydrated through a graded ethanol series to propylene oxide, and embedded in Spurr's resin (Spurr 1969). Serial ultra-thin sections, made with EM UC6 ultramicrotome (Leica, Solms, Germany), were double stained with 2% (w/v) uranyl acetate and lead citrate (Reynolds 1963) and observed using H7600 microscope (Hitachi, Tokyo, Japan).

DNA extraction, PCR amplification, cloning and sequencing

Total DNA was extracted using cetyl trimethylammonium bromide buffer following Kamikawa *et al*. (2009). The nuclear large subunit (LSU) rRNA gene was amplified with forward primer (D1R-F: 5′-ACCCGCTGAATTTAAGCATA-3′; Scholin *et al*. 1994) and reverse primer (D3B-R: 5′-CCTTGGT CCGTGTTTCAAGA-3′; Nunn *et al*. 1996) under the polymerase chain reaction (PCR) conditions described in Lundholm *et al*. (2002). The plastid 16S rRNA gene was amplified by PCR with newly designed forward primer (16SF: 5′-AGAGTTTGATCCTGGCTCAG-3′) and reverse primer (16SR: 5′-TGATCCAACCGCACCTTCCA-3′), under the following PCR conditions: 30 cycles of 95°C for 30 s, 50°C for 30 s, and 72°C for 1 min. Both PCR amplifications were performed using ExTaq (TaKaRa Bio., Ohtsu, Japan) following the manufacturer's instructions. The amplified products were gel-purified and then cloned into pGEMTEasy vector (Promega KK, Tokyo, Japan). The clones were sequenced on both strands. The sequences were deposited in DNA Data Bank of Japan (Table 1).

Molecular phylogenetic analyses

Sequences of the nucleus-encoded LSU rRNA gene were sampled from species/strains in the Bacillariaceae, especially from *Nitzschia* and its closest relatives (Appendix S1 in Supporting Information). We included at least one sequence from each species whose nuclear LSU rRNA gene was available (Appendix S1 in Supporting Information). *N. palea* was reported as a species complex (Trobajo *et al*. 2009), so we included the two *N. palea* sequences that were most distantly related to each other in a previous study (Trobajo *et al*. 2009). Three *Eunotia* species were also added as outgroup taxa because previous phylogenetic analyses (Stepanek & Kociolek 2014) suggested a close relationship between *Eunotia* and the Bacillariaceae. 183 ambiguously aligned nucleotide positions were excluded from the 114-taxon alignment using BioEdit (Hall 1999), leaving 765 unambiguously aligned positions for phylogenetic analyses described below.

Maximum-likelihood (ML) and Bayesian phylogenetic analyses were performed on the LSU rRNA alignment. ML analyses were carried out under the general time reversible (GTR) model incorporating among-site rate variation approximated by a discrete gamma distribution (GTR + Γ model) as the most suitable model for our dataset determined by the program Kakusan4 (Tanabe 2011). ML analyses were performed using RAxML ver. 7.4.4 (Stamatakis 2006) and the ML tree was heuristically searched from 10 distinct parsimony trees. In RAxML bootstrap analyses (100 replicates), the heuristic tree search was performed from a single parsimony tree per replicate. Bayesian analyses were performed under the CAT-GTR + Γ model using PhyloBayes 3.3 (Lartillot *et al*. 2009). Two parallel Markov Chain Monte Carlo runs were run for 39 000 cycles, in which seven million trees and log-likelihoods (lnLs) were sampled. We considered independent runs converged when the maximum discrepancy observed across all bipartitions was 0.05, and effective sample size was >100 (Lartillot *et al*. 2009). The first 10 000 cycles were discarded as burn-in, and trees were summarized to obtain Bayesian posterior probabilities.

Sequences of plastid 16S rRNA gene were sampled from a broad range of lineages in the Bacillariophyceae as well as other algal groups, including cyanobacteria as outgroup taxa (Appendix S2 in Supporting Information). 479 ambiguously aligned nucleotide positions were excluded from the 111-taxon alignment, leaving 1291 unambiguously aligned positions for phylogenetic analyses described below. The GTR + Γ model, which was selected as the most suitable model by Kakusan4 was used for ML analysis. Bayesian analysis was performed as described above with two exceptions: two parallel MCMC were ran for 24 000 cycles, in which 4.5 million trees and lnLs were sampled, and the first 6 000 cycles were discarded as burn-in. We confirmed the maximum discrepancy observed across all bipartitions was 0.08, and effective sample size was >100.

Evaluation of the monophyly of apochlorotic diatoms

In order to evaluate the possible monophyly of the apochlorotic diatoms we used the approximately unbiased (AU) test (Shimodaira 2002). An alternative tree was prepared by constraining the monophyly of all of the apochlorotic diatoms (Table 2; Appendix S3 in Supporting Information). Using the same LSU rRNA alignment, site-wise log-likelihoods (site lnLs) were calculated by RAxML with the GTR + Γ model for the alternative tree and the ML tree. Resultant site lnLs were subsequently analyzed by Consel version 0.1 (Shimodaira & Hasegawa 2001) with the default settings to perform the AU test.

RESULTS

We successfully established 22 culture strains of *Nitzschia* collected from mangrove leaves and water samples (Table 1). These strains were distinguished from photosynthetic diatoms by appearing colorless. Microscopic observations of six

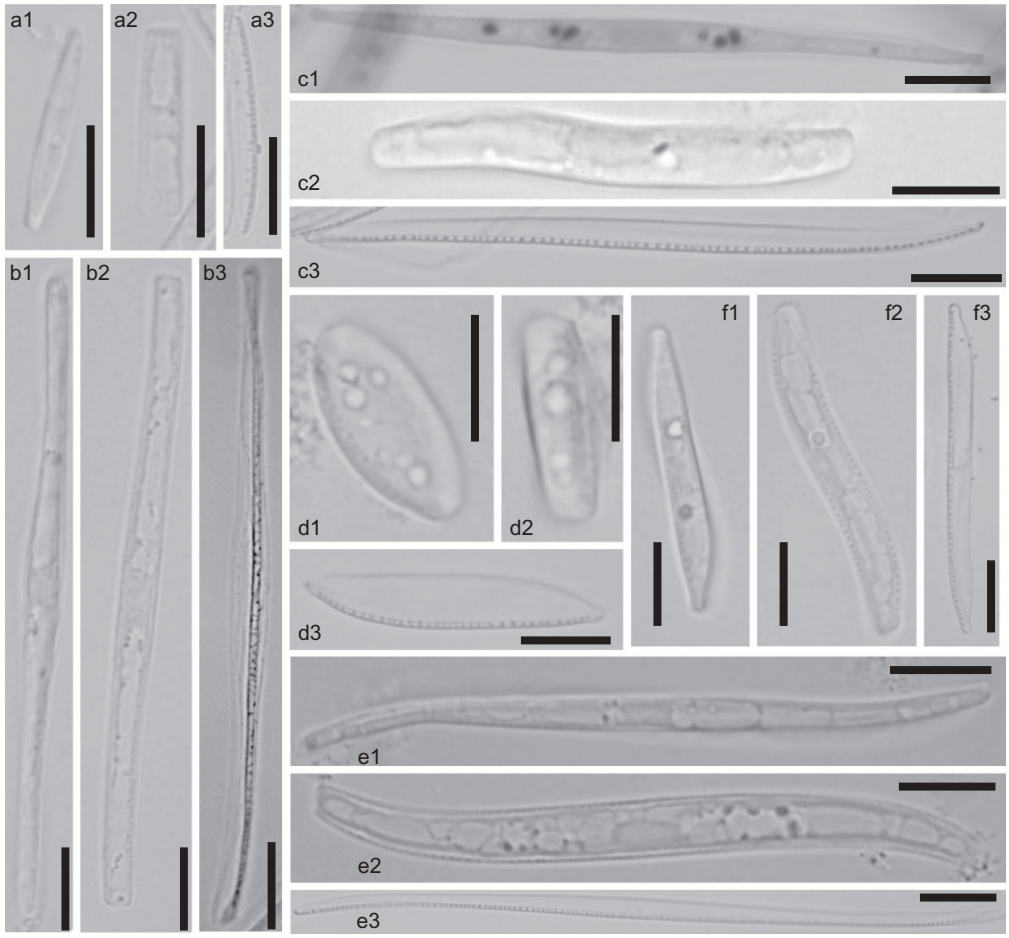

Fig. 1. Light microscopic observations of apochlorotic *Nitzschia* strains. a1–a3: Strain IriIs04, b1–b3: Strain K1, c1–c3: Strain IriSm01, d1–d3: Strain IriSs06, e1–e3: Strain IriSL01, f1–f3: Strain B3. 1: Valve face of a cell, 2: Girdle face of a cell, 3: Valve face of a cleaned frustule. Note that a to f corresponds to morphotype A to F in Figure 2 and Table 1 with C1 (IriSm01) is a cell fixed with the same protocol for TEM whereas the other cells are living. Scale bars show 10 μm.

different strains representing six distinct phylotypes of apochlorotic diatoms (Lineages 1–6, Table 1) in the LSU rRNA phylogeny are shown in Figure 1. The girdle face was rectangular in IriIs04 and IriSs06, and sigmoidal in IriSm01, IriSL01, K1, and B3 (Fig. 1, Table 2). The valve face was lanceolate, wide lanceolate/scalpelliform, fusiform with slightly sigmoid ends, linear with slightly sigmoid ends, fusiform, and linear/scalpelliform in IriIs04, IriSs06, IriSm01, IriSL01, K1, and B3, respectively (Fig. 1, Table 2). Although observations of the precise valve shape in these diatoms were difficult because of vertical undulations of the valve face, the valves were either scalpelliform or almost fusiform to linear with/without sigmoid ends (Table 2). Striae were not observed in all strains, but the keel puncta (fibulae of canal raphe system) were distinctive. The fibulae density was higher in IriIs04 and K1 than that of IriSm01, IriSS06, IriSL01 and B3 (Table 2). A wide gap between central two fibulae, which often reflects the presence of a central nodule in raphe system, was not observed in any of the strains (Fig. 1). We did not find any pigments in these cells (left column in Fig. 2a–f but not shown for all the other strains), which is strongly suggestive of a non-photosynthetic mode of nutrition. When these strains were observed using fluorescence microscopy, although DAPI signals supposedly derived from organellar DNA were observed in addition to those of nucleus (middle column in Fig. 2a–f), no red chlorophyll fluorescence was detected in the cells (right column in Fig. 2a–f).

In order to investigate plastids in our apochlorotic isolates, we characterized the ultrastructure of two strains, IriIs04 and IriSm01. We did not find plastids with conspicuous thylakoids, but instead we observed plastid-like structures with an electron-dense matrix surrounded by four membranes (Fig. 3). The plastid-like structures also possessed a periplastidal compartment positioned between the outer two and inner two membranes (Fig. 3b,d), which is typically seen in the photosynthetic plastids of diatoms. Some of the plastid-like structures in IriIs04 had a few reduced thylakoid-like structures (Fig. 3c).

In order to gain insights into whether the plastid-like structures have retained a genome, we performed PCR-based surveys for the plastid 16S rRNA gene. We determined the sequences of plastid 16S rRNA genes in almost all of the new apochlorotic strains (GenBank accession nos.

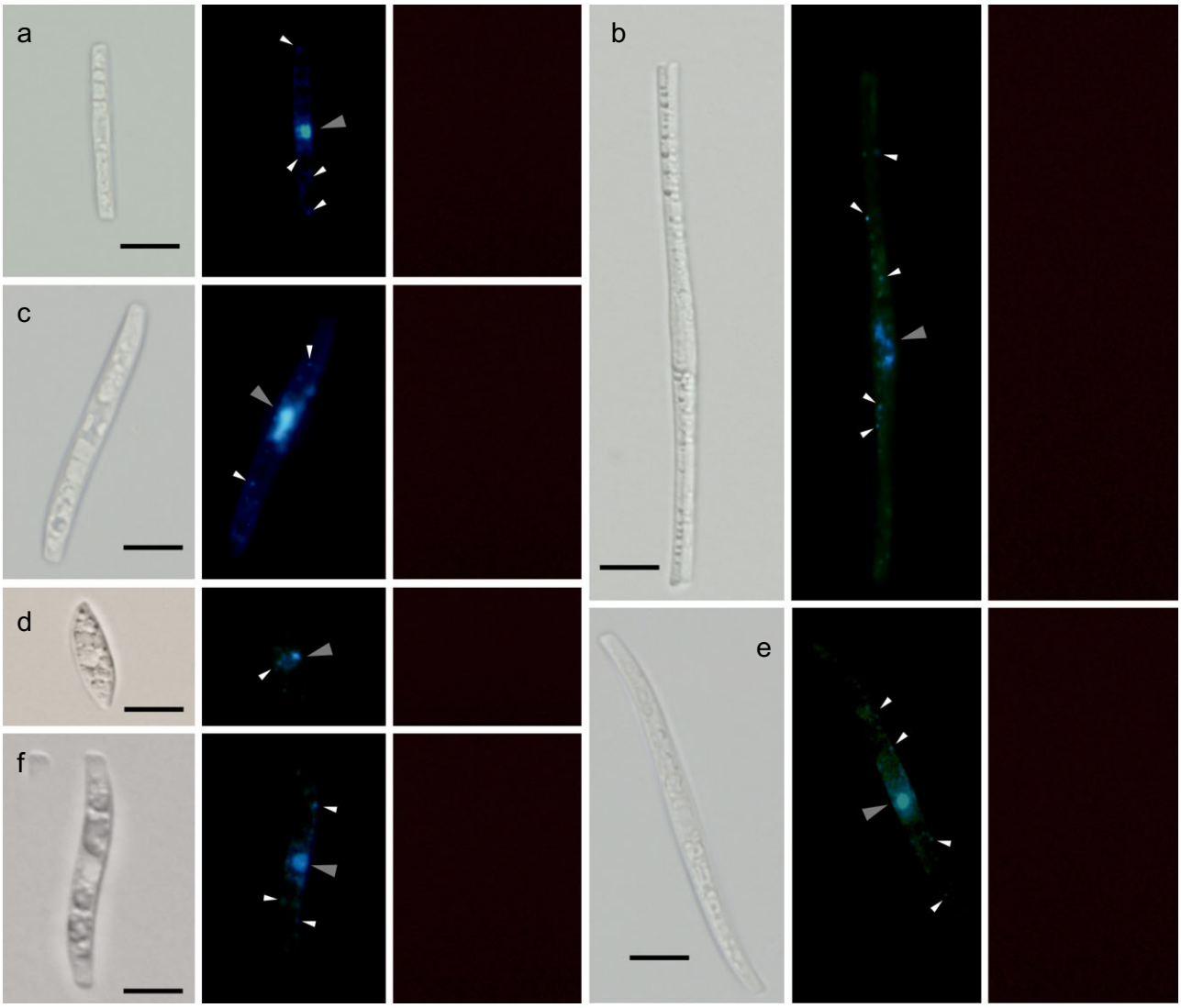

Fig. 2. Fluorescence microscopic observations of apochlorotic *Nitzschia* strains. Left, middle, and right columns show single cells observed under light microscopy, fluorescence microscopy with UV, and fluorescence microscopy with green excitation, respectively. Grey and white arrow heads in the middle columns show DAPI signals derived from nucleus and supposedly derived from organellar genomes, respectively. (a) strain IriIs04; (b) strain K1; (c) strain IriSm01; (d) strain IriSs06; (e) strain IriSL01; (f) strain B3. Note that a to f corresponds to morphotype A to F in Figure 1 and Table 1. Scale bars show 10 μm.

AB899708-AB899728). The branch lengths of the 16S rRNA sequences obtained from the apochlorotic diatoms were much longer than those of photosynthetic species representing a broad range of lineages across the tree of eukaryotes (Fig. 4). In these analyses, the long-branched apochlorotic *Nitzschia* spp. were monophyletic and closely related to the Bacillariaceae (highlighted by stars in Fig. 4).

In order to more rigorously evaluate the phylogenetic relationships among apochlorotic diatoms, we analyzed the 114-taxon alignment consisting of LSU rRNA sequences from the Bacillariaceae, including the previously reported apochlorotic diatoms *Nitzschia alba* (GenBank accession nos. HQ396817 and HQ337473) and *N. leucosigma* (GenBank accession no. HQ396836) (Fig. 5). Our dataset also included the presumed apochlorotic diatom *Nitzschia* sp. CCMP578 (GenBank accession no. HQ396838, see also https://ncma.bigelow.org/ccmp578#.UzPVxfl_tWg). In the LSU rRNA phylogeny (Fig. 5), the apochlorotic diatoms were divided into lineages 1–8. *N. alba* and *Nitzschia* sp. CCMP578 correspond to lineages 7 and 8, respectively. Lineage 6 includes the previously reported sequence of the apochlorotic diatom *N. leucosigma*. The LSU rRNA phylogeny failed to recover the monophyly of lineages 1–8. Nevertheless, lineages 1 and 2, and lineages 3–6 were coalesced into two separate groups with high statistical support. The paraphyletic relationships were not significantly changed if we used other outgroup taxa, such as *Phaeodactylum tricornatum* (GenBank EF553458) and *Pauliella taeniata* (GenBank AF417680) (data not shown).

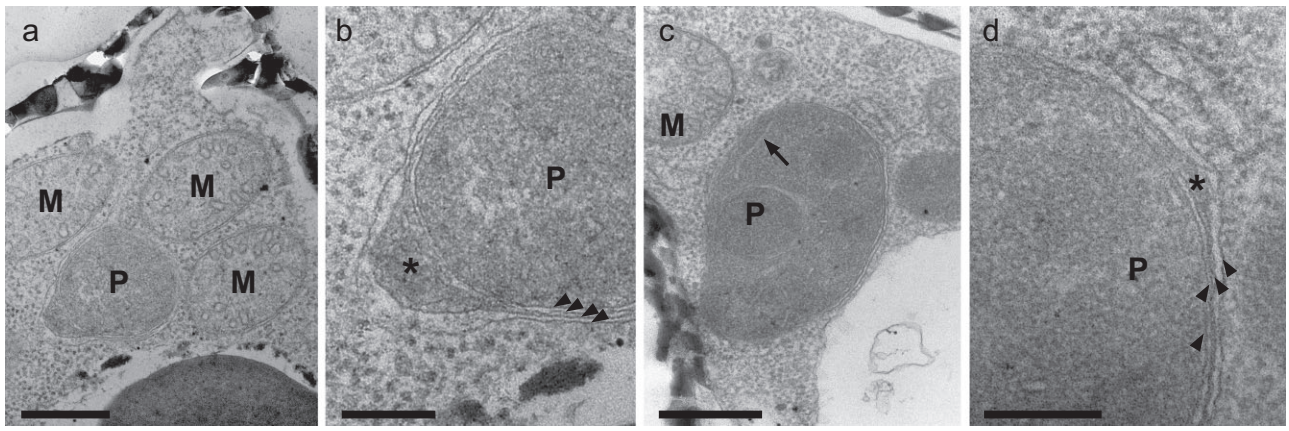

Fig. 3. Transmission electron micrographs of two strains, IriSm01 (a–b) and IriIs04 (c–d) showing details of nonphotosynthetic plastids. (a) Cross section of a nonphotosynthetic plastid (P) and mitochondria (M). (b) High magnification view of the nonphotosynthetic plastid (P) showing four membranes (arrowheads) and a periplastidal compartment (star). (c) Cross section of a nonphotosynthetic plastid (P) and mitochondria (M). Arrow indicates a reduced thylakoid membrane. (d) High magnification view of the nonphotosynthetic plastid showing four membranes (arrowheads) and a periplastidal compartment (star). Scale bars represent 500 nm in a and c and 200 nm in b and d.

In order to assess alternative possibilities regarding the phylogenetic relationships amongst apochlorotic diatom groups (lineages 1–8), an ML tree was inferred after constraining the apochlorotic diatoms as monophyletic (Appendix S3 in Supporting Information). The log likelihood of the alternative tree was only slightly smaller than that of the ML tree (ΔlnL = –9.0). The *P*-value of the alternative tree was 0.313, while that of the ML tree was 0.687. Consequently, the AU test under the 5% *P*-value criterion failed to reject the alternative tree.

DISCUSSION

Light and fluorescence microscopic observations allowed us to conclude that the 22 diatom strains were apochlorotic. Prior to this study, *Nitzschia leucosigma* is the only species that has been formally described as an apochlorotic diatom with a sigmoidal girdle face (Benecke 1900; Lewin & Lewin 1967; Li & Volcani 1987). In this study, we successfully isolated four sigmoidal lineages, and these isolates are distinguishable from *N. leucosigma* in the shape of the valve face: The valve face of *N. leucosigma* is straight (Benecke 1900), while those of morphotypes B, C, E, and F were fusiform, fusiform with a slightly sigmoid end, linear with a slightly sigmoid end, and linear scalpelliform, respectively. The variation in the valve face made it difficult to judge whether sigmoidal apochlorotic isolates in lineages 3, 5, and 6 (corresponding to morphotypes C, E, and F, respectively) are *N. leucosigma*, although they formed a robust clade with *N. leucosigma* in the LSU rRNA phylogeny. On the other hand, sigmoidal apochloritic isolates I4, K1, and K2 (lineage 2/morphotype B) were most likely different from *N. leucosigma* genetically, as the three isolates and *N. leucosigma* were placed in distant positions in the LSU rRNA phylogeny. More detailed morphological characteristics need to be gleaned from the new apochlorotic isolates for their taxonomic treatments in the future.

We observed plastid-like structures without conspicuous thylakoids in strains IriIs04 and IriSm01 and also obtained plastid 16S rRNA sequences from these diatoms, suggesting that the apochlorotic diatoms studied here contain nonphotosynthetic plastids with genomes. This is analogous to those present in apochlorotic euglenids [e.g., *Euglena longa* (Pringsheim) Marin & Melkonian] and cryptomonads [e.g., *Cryptomonas paramecium* (Ehrenberg) Hoef-Emden & Melkonian] (Gockel & Hachtel 2000; Donaher *et al*. 2009). Although metabolic pathway working in nonphotosynthetic plastids of other organisms have been well studied (e.g., apicomplexans, a parasitic green alga, and parasitic land plants; de Koning & Keeling 2004; Wickett *et al*. 2011; Sheiner *et al*. 2013), the metabolic functions of these nonphotosynthetic plastids in apochlorotic diatoms remain unknown, urging us to investigate the roles of the organelle more comprehensively in the future.

The plastid 16S rRNA genes from apochlorotic diatoms are rapidly evolving, and therefore their branches were much longer than other branches in the phylogenetic tree (Fig. 4). Despite similar increments of the evolutionary rates being observed in the genomes of nonphotosynthetic plastids (e.g., Vernon *et al*. 2001), the precise reason for this phenomenon has yet to be elucidated. At least, we conclude that plastid 16S rRNA genes are not ideal to investigate the precise phylogenetic positions of apochlorotic diatoms within the context of diatoms as a whole because of the potential for long-branch attraction (LBA) artefacts (Philippe & Germot 2000; Bergsten 2005). It is known that the impact of LBA artefacts can be reduced when the long branch is ‘split’ by including a sequence (or sequences) closely related to the long-branch sequence of interest (Bergsten 2005). Thus, if one uses plastid 16S rRNA gene sequences to infer the accurate phylogenetic relationships between photosynthetic diatoms and apochlorotic diatoms, it is necessary to acquire more sequence data of other photosynthetic members of the Bacillariaceae, which break the long branches leading to the apochloritic species. Alternatively, nucleotide substitution

Fig. 4. Maximum-likelihood tree of plastids inferred from plastid 16S rRNA gene sequences. Only bootstrap values over 70% are shown. Nodes supported by Bayesian posterior probabilities over 0.95 are shown by thick branches. Closed stars show taxa that belong to the Bacillariaceae. The labels 1 to 6 for apochlorotic diatom lineages correspond to those in Figure 5 and phylotype 1 to 6 in Table 1.

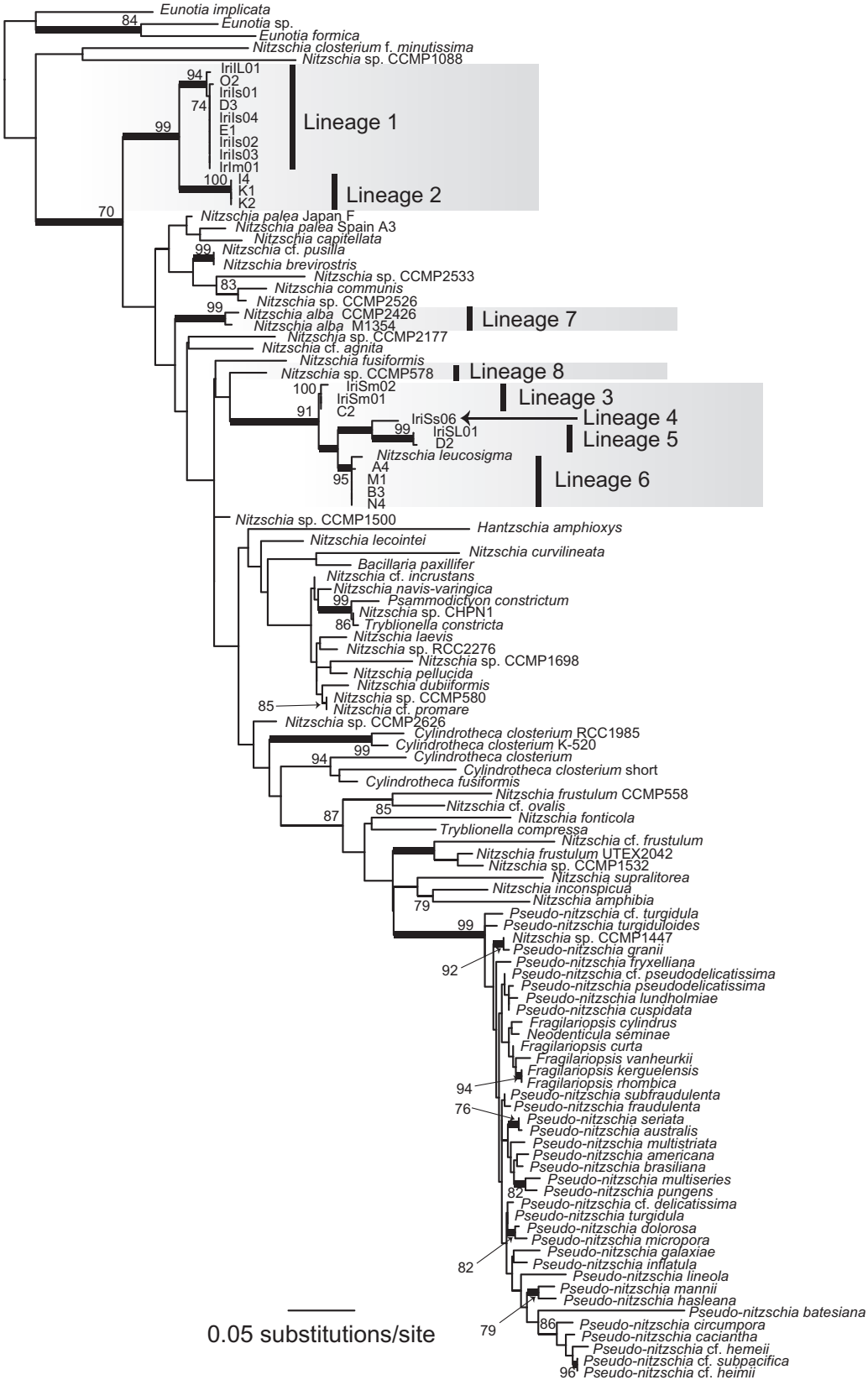

Fig. 5. Maximum-likelihood tree of *Nitzschia* and its close relatives as inferred from large subunit rRNA gene sequences. Taxa were broadly sampled from the Bacillariaceae. Apochlorotic diatoms are shaded in grey. Other information is the same as Figure 4.

models, in which tempo and mode of sequence evolution can be varied across subtrees, might help overcome LBA artefacts (e.g., Ishikawa *et al*. 2012).

In contrast to plastid 16S rRNA genes, nuclear LSU rRNA genes are likely more suitable for phylogenetic analyses to investigate the phylogenetic positions of apochlorotic diatoms because the branch lengths are not significantly longer than other species. The analyses of LSU rRNA sequences showed apochlorotic diatoms divided into eight distinct lineages that did not form a clade. This polyphyletic distribution of apochlorotic diatoms suggests that loss of photosynthetic ability has occurred several times independently within *Nitzschia*; however, the monophyly of these lineages was not confidently rejected by a statistical test. This possibility can be tested by additional analyses using other phylogenetic markers.

Several lineages of eukaryotes have lost their photosynthetic ability, such as some species of cryptomonads (Sepsenwol 1973; Hoef-Emden 2005), euglenids (e.g., Gockel & Hachtel 2000; Triemer & Farmer 2007), green algae (e.g., Menke & Ericke 1962; Leliaert *et al*. 2012), stramenopiles (e.g., Sekiguchi *et al*. 2002; Yubuki *et al*. 2008) and alveolates (e.g., Cavalier-Smith 2002; Fernández Robledo *et al*. 2011). The independent loss of photosynthesis in distantly related lineages of eukaryotes suggests that this evolutionary pattern has also helped shape the current patchy distribution of photosynthetic species across the tree of eukaryotes. Therefore, it is intriguing to understand the evolutionary force behind the loss of photosynthesis. *Nitzschia* is one of the most species-rich and successful eukaryotic lineages in both oceanic and freshwater environments. Yet, several *Nitzschia* lineages likely have experienced secondary loss of photosynthesis. Some species of diatoms including photosynthetic *Nitzschia* spp. are known to grow under dark conditions by utilizing dissolved organic carbon (Hellebust & Lewin 1977). This suggests that some, if not all, species of diatoms have a mechanism for carbon uptake; however, to our knowledge, genes and proteins associated with this mechanism have not been reported. The origin(s) and subsequent maintenance of mixotrophy may have, at least in part, allowed some *Nitzschia* species to lose photosynthesis under certain conditions. For instance, it may be possible to gain carbon-sources through interactions with the surfaces of macroalgae and mangrove leaves: these are common associations in the isolates of apochlorotic diatoms that have been described so far (Lewin & Lewin 1967; Li & Volcani 1987; this study). If so, apochlorotic diatom species may not be restricted to *Nitzschia* and *Hantzschia* because mixotrophy has been reported from many other genera of diatoms (e.g., *Melosira*, *Navicula*, *Cylindrotheca*, and *Cocconeisis*; Hellebust & Lewin 1977). It is also certainly possible that future discoveries will demonstrate new non-photosynthetic species that are more distantly related to *Nitzschia*.

ACKNOWLEDGMENTS

We thank Professor Isao Inouye (University of Tsukuba, Japan) for providing some environmental samples. This work was supported in part by a grant from the Institute for Fermentation, Osaka, Japan (awarded to RK) and those from JSPS awarded to RK (no. 24870004), MY (no. 23770234), YI (nos. 22657025 and 23117006) and TH (nos. 23117001A, 23117005A, 23247038, and 23405013). This research was also supported in part by grants from the Tula Foundation (Centre for Microbial Diversity and Evolution), the National Science and Engineering Research Council of Canada (NSERC 2014-05258), and the Canadian Institute for Advanced Research, Program in Integrated Microbial Biodiversity to BSL.

REFERENCES

Anderson, D. M. 1989. Toxic algal blooms and red tides: a global perspective. *In* Okaichi, T., Anderson, D. M. and Nemoto, T. (Eds) *Red Tides: Biology, Environmental Science and Toxicology*. Elsevier, New York, pp. 11–6.

Benecke, W. 1900. Über farblose diatomeen der Kieler Föhrde. *Jahrb. Wiss. Bot.* **35**: 535–72.

Bergsten, J. 2005. A review of long-branch attraction. *Cladistics* **21**: 163–93.

Blackburn, M. V., Hannah, F. and Rogerson, A. 2009a. First account of apochlorotic diatoms from mangrove waters in Florida. *J. Eukaryot. Microbiol*. **56**: 194–200.

Blackburn, M. V., Hannah, F. and Rogerson, A. 2009b. First account of apochlorotic diatoms from intertidal sand of a south Florida beach. *Estuar. Coast. Shelf Sci*. **84**: 519–26.

Cavalier-Smith, T. 2002. Chloroplast evolution: secondary symbiogenesis and multiple losses. *Curr. Biol.* **12**: R62–4.

Daugbjerg, N. and Guillou, L. 2001. Phylogenetic analyses of Bolidophyceae (Heterokontophyta) using *rbcL* gene sequences support their sister group relationship to diatoms. *Phycologia* **40**: 153–61.

de Koning, A. P. and Keeling, P. J. 2004. Nucleus-encoded genes for plastid-targeted proteins in *Helicosporidium*: functional diversity of a cryptic plastid in a parasitic alga. *Eukaryot. Cell* **3**: 1198–205.

Donaher, N., Tanifuji, G., Onodera, N. T. *et al*. 2009. The complete plastid genome sequence of the secondarily nonphotosynthetic alga *Cryptomonas paramecium*: reduction, compaction, and accelerated evolutionary rate. *Genome Biol. Evol*. **1**: 439–48.

Fernández Robledo, J. A., Calerb, E., Matsuzaki, M. *et al*. 2011. The search for the missing link: a relic plastid in *Perkinsus*? *Int. J. Parasitol*. **41**: 1217–29.

Field, C. B., Behrenfeld, M. J., Randerson, J. T. and Falkowski, P. 1998. Primary production of the biosphere: integrating terrestrial and oceanic components. *Science* **281**: 237–40.

Geitler, L. 1968. Die Lage der Raphen in den Zellen von *Nitzschia*-Arten. *Ber. Deutsch. Bot. Ges.* **81**: 411–3.

Gockel, G. and Hachtel, W. 2000. Complete gene map of the plastid genome of the nonphotosynthetic euglenoid flagellate *Astasia longa*. *Protist* **151**: 347–51.

Hall, T. A. 1999. BioEdit: a user friendly biological sequence alignment editor and analysis program for windows 95/98/NT. *Nucleic Acids Symp. Ser.* **41**: 95–8.

Hallegaeff, G. M. 1993. A review of harmful algal blooms and their apparent global increase. *Phycologia* **32**: 79–99.

Hellebust, J. A. and Lewin, J. 1977. Heterotrophic nutrition. *In* Werner, D. (Ed.) *The Biology of Diatoms*. University of California Press, Berkeley and Los Angeles, pp. 169–97.

Hoef-Emden, K. 2005. Multiple independent losses of photosynthesis and differing evolutionary rates in the genus *Cryptomonas* (Cryptophyceae): combined phylogenetic analyses of DNA sequences of the nuclear and the nucleomorph ribosomal operons. *J. Mol. Evol.* **60**: 183–95.

Ishikawa, S. A., Inagaki, Y. and Hashimoto, T. 2012. RY-coding and non-homogeneous models can ameliorate the maximum-likelihood

inferences from nucleotide sequence data with parallel compositional heterogeneity. *Evol. Bioinform. Online* **8**: 357–71.
Kamikawa, R., Nishiura, H. and Sako, Y. 2009. Analysis of the mitochondrial genome, transcripts, and electron transport activity in the dinoflagellate *Alexandrium catenella* (Gonyaulacales, Dinophyceae). *Phycol. Res.* **57**: 1–11.
Kasai, F., Kawachi, M., Erata, M. *et al.* 2009. NIES-collection list of strains, 8th edition. *Jpn. J. Phycol. (Sorui)* **57** (Suppl.): 1–350.
Lartillot, N., Lepage, T. and Blanquart, S. 2009. PhyloBayes 3: a Bayesian software package for phylogenetic reconstruction and molecular dating. *Bioinformatics* **25**: 2286–8.
Lauritis, J. A., Hemmingsen, B. B. and Volcani, B. E. 1967. Propagation of *Hantzschia* sp. Grunow daughter cells by *Nitzschia alba* Lewin and Lewin. *J. Phycol.* **3**: 236–7.
Lauritis, J. A., Coombs, J. and Volcani, B. E. 1968. Studies on the biochemistry and fine structure of silica shell formation in diatoms. IV. Fine structure of the apochlorotic diatom *Nitzschia alba* Lewin & Lewin. *Arch. Miklobiol.* **62**: 1–16.
Leliaert, F., Smith, D. R., Moreau, H. *et al.* 2012. Phylogeny and molecular evolution of the green algae. *Crit. Rev. Plant Sci.* **31**: 1–46.
Lewin, J. C. and Lewin, R. A. 1967. Culture and nutrition of some apochlorotic diatoms of the genus *Nitzschia*. *J. Gen. Microbiol.* **46**: 361–7.
Li, C. W. and Volcani, B. E. 1987. Four new apochlorotic diatoms. *Br. Phycol. J.* **22**: 375–82.
Lundholm, N., Daugbjerg, N. and Moestrup, Ø. 2002. Phylogeny of the Bacillariaceae with emphasis on the genus *Pseudo-nitzschia* (Bacillariophyceae) based on partial LSU rDNA. *Eur. J. Phycol.* **37**: 115–34.
Mann, D. G. 1980. *Hantzschia fenestrata* Hust. (Bacillariophyta) – *Hantzschia* or *Nitzschia*? *Br. Phycol. J.* **15**: 249–60.
Mann, D. G. 1999. The species concept in diatoms. *Phycologia* **38**: 437–95.
Menke, W. and Ericke, B. 1962. Einige Beobachtungen an *Prototheca ciferrii*. *Port. Acta Biol. A* **6**: 243–52.
Nagumo, T. 1995. Simple and safe cleaning methods for diatom samples. *Diatom* **10**: 88.
Nunn, G. B., Theisen, B. F., Christensen, B. and Arctander, P. 1996. Simplicity-correlated size growth of the nuclear 28S ribosomal RNA D3 expansion segment in the crustacean order Isopoda. *J. Mol. Evol.* **42**: 211–23.
Philippe, H. and Germot, A. 2000. Phylogeny of eukaryotes based on ribosomal RNA: long-branch attraction and models of sequence evolution. *Mol. Biol. Evol.* **17**: 830–4.
Pickett-Heaps, J. 1983. Valve morphogenesis and the microtubule center in three species of the diatom *Nitzschia*. *J. Phycol.* **19**: 269–81.
Porter, K. G. and Feig, Y. S. 1980. The use of DAPI for identifying and counting aquatic microflora. *Limnol. Oceanogr.* **25**: 943–8.
Reynolds, E. S. 1963. The use of lead citrate at high pH as an electron-opaque stain in electron microscopy. *J. Cell Biol.* **17**: 208–12.
Schnepf, E. 1969. Leukoplasten bei *Nitzschia alba*. *Oesterr. Bot. Z.* **116**: 65–9.
Scholin, C. A., Herzog, M., Sogin, M. and Anderson, D. M. 1994. Identification of group- and strain-specific genetic markers for globally distributed *Alexandrium* (Dinophyceae). II. Sequence analysis of a fragment of the LSU rDNA. *J. Phycol.* **30**: 999–1011.
Sekiguchi, H., Moriya, M., Nakayama, T. and Inouye, I. 2002. Vestigial chloroplasts in heterotrophic Stramenopiles *Pteridomonas danica* and *Ciliophrys infusionum* (Dictyochophyceae). *Protist* **153**: 157–67.
Sepsenwol, S. 1973. Leucoplast of the cryptomonad *Chilomonas paramecium*. *Exp. Cell Res.* **76**: 395–409.
Sheiner, L., Vaidya, A. B. and McFadden, G. I. 2013. The metabolic roles of the endosymbiotic organelles of *Toxoplasma* and *Plasmodium* spp. *Curr. Opin. Microbiol.* **16**: 452–8.
Shimodaira, H. 2002. An approximately unbiased test of phylogenetic tree selection. *Syst. Biol.* **51**: 492–508.
Shimodaira, H. and Hasegawa, M. 2001. CONSEL: for assessing the confidence of phylogenetic tree selection. *Bioinformatics* **17**: 1246–7.
Spurr, A. R. 1969. A low-viscosity epoxy resin embedding medium for electron microscopy. *J. Ultrastruct. Res.* **26**: 31–43.
Stamatakis, A. 2006. RAxML-VI-HPC: maximum likelihood-based phylogentic analyses with thousands of taxa and mixed models. *Bioinfomatics* **22**: 2688–90.
Stepanek, J. G. and Kociolek, J. P. 2014. Molecular phylogeny of *Amphora* sensu lato (Bacillariophyta): an investigation into the monophyly and classification of the amphoroid diatoms. *Protist* **165**: 177–95.
Tanabe, A. S. 2011. Kakusan4 and Aminosan: two programs for comparing nonpartitioned, proportional, and separate models for combined molecular phylogenetic analyses of multilocus sequence data. *Mol. Ecol. Res.* **11**: 914–21.
Triemer, R. E. and Farmer, M. A. 2007. A decade of euglenoid molecular phylogenetics. *In* Brodie, J. and Lewis, J. (Eds) *Unravelling the Algae: The Past, Present, and Future of Algal Systematics*. The Systematics Association Special Volume Series 75, CRC Press, Boca Raton, pp. 315–30.
Trobajo, R., Clavero, E., Chepurnov, V. A. *et al.* 2009. Morphological, genetic and mating diversity within the widespread bioindicator *Nitzschia palea* (Bacillariophyceae). *Phycologia* **48**: 443–59.
Vernon, D., Gutell, R. R., Cannone, J. J., Rumpf, R. W. and Birky, C. W. Jr. 2001. Accelerated evolution of functional plastid rRNA and elongation factor genes due to reduced protein synthetic load after the loss of photosynthesis in the chlorophyte alga *Polytoma*. *Mol. Biol. Evol.* **18**: 1810–22.
Watanabe, T., Kodama, Y. and Mayama, S. 2010. Application of a novel cleaning method using low-temperature plasma on tidal flat diatoms with heterovalvy or delicate frustule structure. *Proc. Natl. Acad. Sci. Philad.* **160**: 83–7.
Wickett, N. J., Honaas, L. A., Wafula, E. K. *et al.* 2011. Transcriptomes of the parasitic plant family Orobanchaceae reveal surprising conservation of chlorophyll synthesis. *Curr. Biol.* **21**: 2098–104.
Yubuki, N., Nakayama, T. and Inouye, I. 2008. A unique life cycle and perennation in a colorless chrysophyte *Spumella* sp. *J. Phycol.* **44**: 164–72.

SUPPORTING INFORMATION

Additional Supporting Information may be found in the online version of this article at the publisher's web-site:

Appendix S1. Nuclear LSU rRNA gene sequences used in this study.
Appendix S2. Plastid 16S rRNA gene sequences used in this study.
Appendix S3. ML tree inferred after constraining the apochlorotic diatoms as monophyletic.